Faraday Discussions

Cite this: *Faraday Discuss.*, 2021, **226**, 290

PAPER

View Article Online
View Journal | View Issue

Open Access Article. Published on 23 2020. Downloaded on 09-10-2024 6:25:25.
This article is licensed under a Creative Commons Attribution 3.0 Unported Licence.

An evaluation of source apportionment of fine OC and $PM_{2.5}$ by multiple methods: APHH-Beijing campaigns as a case study†

Jingsha Xu, [a] Deepchandra Srivastava,[a] Xuefang Wu,[ab] Siqi Hou,[ac] Tuan V. Vu,‡[a] Di Liu,[ad] Yele Sun, [d] Athanasia Vlachou,[e] Vaios Moschos, [e] Gary Salazar,[f] Sönke Szidat,[f] André S. H. Prévôt,[e] Pingqing Fu, [dg] Roy M. Harrison §*[a] and Zongbo Shi *[a]

Received 17th July 2020, Accepted 3rd August 2020
DOI: 10.1039/d0fd00095g

This study aims to critically evaluate the source apportionment of fine particles by multiple receptor modelling approaches, including carbon mass balance modelling of filter-based radiocarbon (^{14}C) data, Chemical Mass Balance (CMB) and Positive Matrix Factorization (PMF) analysis on filter-based chemical speciation data, and PMF analysis on Aerosol Mass Spectrometer (AMS-PMF) or Aerosol Chemical Speciation Monitor (ACSM-PMF) data. These data were collected as part of the APHH-Beijing (Atmospheric Pollution and Human Health in a Chinese Megacity) field observation campaigns from 10th November to 12th December in winter 2016 and from 22nd May to 24th June in summer 2017. ^{14}C analysis revealed the predominant contribution of fossil fuel combustion to carbonaceous aerosols in winter compared with non-fossil fuel sources, which is supported by the results from other methods. An extended Gelencsér (EG) method incorporating ^{14}C data, as well as the CMB and AMS/ACSM-PMF methods, generated a consistent source apportionment for fossil fuel related primary organic carbon. Coal combustion, traffic and biomass burning POC were comparable for CMB and AMS/

[a]*School of Geography, Earth and Environmental Sciences, University of Birmingham, Birmingham, B15 2TT, UK. E-mail: Z.Shi@bham.ac.uk; r.m.harrison@bham.ac.uk*

[b]*School of Geology and Mineral Resources, China University of Geosciences, Xueyuan Road 29, 100083, Beijing, China*

[c]*State Key Laboratory for Structural Chemistry of Unstable and Stable Species, Beijing National Laboratory for Molecular Sciences (BNLMS), Institute of Chemistry, Chinese Academy of Sciences, Beijing, 100190, China*

[d]*Institute of Atmospheric Physics, Chinese Academy of Sciences, Beijing, 100029, China*

[e]*Laboratory of Atmospheric Chemistry, Paul Scherrer Institute, Villigen PSI, CH-5232, Switzerland*

[f]*Department of Chemistry and Biochemistry & Oeschger Centre for Climate Change Research, University of Bern, 3012 Bern, Switzerland*

[g]*Institute of Surface-Earth System Science, School of Earth System Science, Tianjin University, Tianjin, China*

† Electronic supplementary information (ESI) available. See DOI: 10.1039/d0fd00095g

‡ Now at: School of Public Health, Imperial College London, W2 1PG, UK.

§ Also at: Department of Environmental Sciences/Center of Excellence in Environmental Studies, King Abdulaziz University, P.O. Box 80203, Jeddah, 21589, Saudi Arabia.

 This journal is © The Royal Society of Chemistry 2021

ACSM-PMF. There are uncertainties in the EG method when estimating biomass burning and cooking OC. The POC from cooking estimated by different methods was poorly correlated, suggesting a large uncertainty when differentiating this source type. The $PM_{2.5}$ source apportionment results varied between different methods. Through a comparison and correlation analysis of CMB, PMF and AMS/ACSM-PMF, the CMB method appears to give the most complete and representative source apportionment of Beijing aerosols. Based upon the CMB results, fine aerosols in Beijing were mainly secondary inorganic ion formation, secondary organic aerosol formation, primary coal combustion and from biomass burning emissions.

Open Access Article. Published on 23 2020. Downloaded on 09-10-2024 6:25:25.
This article is licensed under a Creative Commons Attribution 3.0 Unported Licence.

1. Introduction

Fine particulate matter ($PM_{2.5}$) has adverse effects on atmospheric visibility and human health, and influences the climate.[1,2] In Beijing, $PM_{2.5}$ pollution remains a major challenge with its hourly concentration reaching as high as 438 $\mu g\ m^{-3}$ during the APHH-Beijing (Atmospheric Pollution and Human Health in a Chinese Megacity) winter campaign.[3] Source apportionment of $PM_{2.5}$ provides important information for developing more effective pollution control strategies.

Receptor modelling methods such as Positive Matrix Factorization (PMF), Chemical Mass Balance (CMB) and UNMIX have been widely applied for the source apportionment of $PM_{2.5}$.[4] For the CMB model, aerosol chemical composition data from the sources and the receptor site are needed. It constructs the best-fit linear combination of the chemical compositions of source profiles to match the ambient particle composition.[5] The selection of source profiles requires a good understanding of the likely sources contributing to PM at the sampling site. The CMB model can provide the most reliable results when each source is well characterized with a constant chemical composition. The inherent uncertainties in using this model derive mainly from errors in the measurement of chemical species and the selection of source profiles. If the source profile is unrepresentative or not included, then the source apportionment results are less trustworthy. CMB has been applied in many studies and has been confirmed to be a good tool for apportioning primary sources of carbonaceous aerosols.[6,7]

PMF is a receptor model which does not require any prior information about source profiles. It is a bilinear unmixing model which assumes that its dataset matrix comprises a linear combination of factors.[8] The factor profiles should be constant and varied in species concentrations with all values constrained to be positive in the model. The number of factors is not fixed, and the modeler needs to select the optimal number of factors for the best interpretation of the data. This is considered as the least quantitative step in PMF analysis, as it largely depends on subjective judgements and the skills of the user.[9,10] In addition, linear transformations (rotations) of the factors may also complicate the results and increase the uncertainties. Brown *et al.*[11] reported methods for estimating the uncertainties in PMF solutions. Another shortcoming of the PMF method is that it requires a large number of samples for analysis, while CMB can be applied to only a few ambient samples, and in theory even a single sample.

In addition to the application of PMF to datasets from integrated air samples, PMF can also be applied to continuous Aerodyne Aerosol Mass Spectrometer (AMS) or Aerosol Chemical Speciation Monitor (ACSM) datasets (AMS/ACSM-

Open Access Article. Published on 23 2020. Downloaded on 09-10-2024 6:25:25.
This article is licensed under a Creative Commons Attribution 3.0 Unported Licence.

PMF). AMS and ACSM are widely applied to characterize the chemical species in submicron non-refractory particles ($NR\text{-}PM_1$) with high time resolution.[12–14] Unlike some atmospheric datasets which include OC/EC, metals and inorganic ions, measured by multiple instruments, an advantage of AMS/ACSM-PMF is that the measurement error is more coherent as the data were obtained from a single instrument. However, these online datasets are also accompanied by uncertainties in the determination of the relative ionisation efficiencies (RIEs) and collection efficiencies (CEs).[15] Accurate knowledge of RIEs and CEs is important for quantification, and this information is not always available.[16] Through investigation of the dominant peaks at representative m/z resulting from significant fragmentation following vaporization and ionization in the AMS/ACSM, organic aerosol (OA) sources including primary (coal combustion, biomass burning, traffic, cooking) and generic secondary sources can be identified by PMF factor analysis.[8,13] However, it is reported that AMS/ACSM-PMF has difficulty separating cooking and vehicular emissions as they share similar mass spectra.[17–19]

^{14}C analysis has been widely applied for the differentiation of fossil and non-fossil sources of carbonaceous aerosols.[20–22] It can quantitatively differentiate atmospheric carbonaceous aerosols from fossil fuels and from contemporary biomass, as fossil fuels are devoid of ^{14}C while modern biomass carbon has a well-recognized $^{14}C/^{12}C$ ratio.[23] The advantage of this approach is that this ratio is an intrinsic property of the carbonaceous aerosol, which is independent of concentration, unlike molecular tracers.[23] It is considered as a robust method to unambiguously distinguish fossil and non-fossil sources of carbonaceous particles.[21,24] The disadvantage is that ^{14}C measurements are mainly conducted on total carbon (TC), organic carbon (OC) and elemental carbon (EC), and they require a large mass of sample to be analysed in order to apportion specific compounds like PAHs or fatty acids.[25,26] ^{14}C measurements can be combined with molecular tracers (*i.e.* levoglucosan for biomass burning, arabitol/mannitol for fungal spores), and OC/EC emission ratios from the literature for distinguishing natural or anthropogenic or more specific sources.[27,28]

Since each method has its own uncertainties and limitations for source apportionment, it is important to compare the results from different methods in order to better understand the source apportionment results. Szidat *et al.* (2018)[29] combined the results from ^{14}C analysis with those from AMS-PMF, and quantified fossil and non-fossil secondary organic aerosols (SOAs). Ke *et al.* (2007)[30] compared ^{14}C and CMB results and found comparable results for fossil and contemporary source-derived primary carbon. Huang *et al.* (2013)[31] found good correlation for the SOAs estimated from the OC/EC ratios and those estimated by AMS-PMF in summer, but the OC/EC method overestimated SOAs in winter due to more biomass burning activities. Yin *et al.*[4] compared CMB and AMS-PMF results and found a generally good correlation between the two methods, but the contributions of some individual organic aerosol sources were different. Bullock *et al.*[32] apportioned the sources of PM by applying both CMB and PMF to the same dataset, suggesting that the model results are strongly affected by the selection of molecular tracers and source profiles. Most of the comparisons so far were only done between two methods.

Open Access Article. Published on 23 2020. Downloaded on 09-10-2024 6:25:25.
This article is licensed under a Creative Commons Attribution 3.0 Unported Licence.

In this study, we provide a critical comparative evaluation of the source apportionment results from multiple RM methods applied to a dataset generated from the APHH-Beijing field campaigns in Beijing as a case study.

2. Methodology

2.1 Field campaigns

$PM_{2.5}$ samples were collected at an urban site and a rural site in Beijing during winter (10th November to 12th December 2016) and summer (22nd May to 24th June 2017) campaigns as part of the APHH-Beijing programme.[3] The urban site (39.98 N, 116.39 E) is located at the Institute of Atmospheric Physics (IAP), Chinese Academy of Sciences in Beijing, China, while the rural site (40.17 N, 117.05 E) is in a village in Pinggu (PG) District. An AMS was deployed at the urban site during both campaigns and an ACSM was deployed at the rural site in winter only. The details of this field campaign can be found elsewhere.[3,33]

2.2 Offline sample analyses

$PM_{2.5}$ samples were characterized by IC for inorganic ions, ICP-MS for trace metals, XRF for crustal elements, a DRI2015 analyzer for OC and EC, and GC-MS for organic tracers. The ^{14}C in total carbon (TC), EC and water insoluble OC was determined for 13 IAP samples and 12 PG samples by using an accelerator mass spectrometer.[34,35] More details of the analytical methods are given in the ESI† and elsewhere.[36,37]

2.3 Extended Gelencsér (EG) method

The method of Gelencsér *et al.* (2007)[38] was developed further to incorporate radiocarbon data for source apportionment of OC and EC from biomass burning, cooking and secondary organic aerosols. In Hou *et al.* (2020),[39] the ^{14}C results were combined with the OC/EC ratios in different sources to apportion the OC into primary OC from fossil fuels, biomass burning and cooking, and secondary OC, and this method is referred to as the extended Gelencsér (EG) method. The uncertainties of the EG method mainly come from measurement errors and the inferred constituent ratios like OC/EC for different sources. Details of the Gelencsér method and the extended Gelencsér method are provided in Table S1.†

2.4 Chemical mass balance (CMB) modelling

A receptor model – the chemical mass balance (US EPA CMB8.2) – was applied for fine OC source apportionment. CMB modelling for the IAP and PG sites was conducted separately using the same source profiles mainly obtained from China. Experimental details are provided in Xu *et al.* (2020)[36] and Wu *et al.* (2020)[37] for IAP and PG, respectively.

2.5 Positive matrix factorization (PMF) modelling

PMF modelling was conducted both for filter-based data and for online AMS data and ACSM data.[8,40] For filter-based data, 133 samples from both sites in winter and summer were combined for PMF modelling. The AMS and ACSM data

Open Access Article. Published on 23 2020. Downloaded on 09-10-2024 6:25:25.
This article is licensed under a Creative Commons Attribution 3.0 Unported Licence.

Table 1 Average $PM_{2.5}$, OC and EC concentrations ($\mu g\ m^{-3}$) at the IAP and PG sites during winter and summer

Sampling period	IAP winter ($n = 33$) 10th November to 12th December, 2016	IAP summer ($n = 34$) 23rd May to 25th June, 2017	PG winter ($n = 32$) 10th November to 11th December, 2016	PG summer ($n = 34$) 22nd May to 24th June, 2017
$PM_{2.5}/\mu g\ m^{-3}$	91.6 ± 63.7 (10.3–239.9)	30.2 ± 14.8 (12.2–78.8)	99.7 ± 77.8 (13.3–294.3)	27.5 ± 12.9 (11.6–70.3)
$OC/\mu g\ m^{-3}$	20.9 ± 12.2 (3.9–48.8)	6.4 ± 2.3 (1.8–12.7)	33.2 ± 22.0 (3.8–85.0)	7.7 ± 3.4 (1.8–17.9)
$EC/\mu g\ m^{-3}$	3.4 ± 2.0 (0.3–6.6)	0.9 ± 0.4 (0.2–1.7)	3.7 ± 2.3 (0.3–9.8)	1.2 ± 0.7 (0.1–3.1)

 This journal is © The Royal Society of Chemistry 2021

Open Access Article. Published on 23 2020. Downloaded on 09-10-2024 6:25:25.
This article is licensed under a Creative Commons Attribution 3.0 Unported Licence.

analysis details are described elsewhere.[14] The application of PMF to speciated chemical data from off-line filter samples is described by Srivastava *et al.* (2020).[41]

3. Results and discussion

3.1 $PM_{2.5}$, OC and EC concentrations

The average $PM_{2.5}$ concentrations in winter were 91.6 ± 63.7 and 99.7 ± 77.8 μg m^{-3} at the IAP and PG sites, respectively, and those in summer were 30.2 ± 14.8 and 27.5 ± 12.9 μg m^{-3} at the IAP and PG sites, respectively (Table 1). During the winter campaign, 18 and 15 haze days ($PM_{2.5} \geq 75$ μg m^{-3}) were observed at the IAP and PG sites, respectively. In summer, one haze day was observed at the IAP site on 27th May 2017, with a $PM_{2.5}$ concentration of 78.8 μg m^{-3}. OC contributed 26.5 ± 8.5% and 23.3 ± 7.6% of $PM_{2.5}$ in winter and summer, respectively at the IAP site, and 39.0 ± 15.9% and 30.3 ± 11.4% of $PM_{2.5}$ in winter and summer, respectively at the PG site. In winter, TC (OC + EC) contributed 30.6 ± 9.5% and 43.6 ± 18.1% of $PM_{2.5}$ at the IAP and PG sites, respectively, highlighting the importance of understanding the sources of carbonaceous aerosols at both sites.

3.2 Comparison of OC source apportionment results by different methods

The contribution of fossil and non-fossil sources to TC, OC and EC was analysed through ^{14}C analysis (Fig. S1†). Generally, non-fossil fuel sources accounted for 41% of TC, which is comparable with the percentage reported in another study conducted in Beijing (45%).[42] The concentration of non-fossil fuel derived OC (OC_{nf}) was 19.7 ± 11.5 μg m^{-3} at PG in winter, more than two times that at IAP in winter (8.6 ± 4.7 μg m^{-3}), while for OC_{nf} in summer, the two sites were not significantly different. The concentration of fossil fuel derived OC (OC_f) was much higher than that of OC_{nf} in winter, while the concentration of OC_f in summer was close to that of OC_{nf} at both sites.

The extended Gelencsér method further separated OC into POC_{nf}, POC_f, SOC_{nf} and SOC_f. POC_{nf} was also separated into biomass burning (POC_{bb}) and cooking (POC_{ck}). However, due to the limited number of samples used for ^{14}C analysis, the results from the EG method may not be representative of the whole sampling period. Hence, we compared the source apportionment results from CMB, PMF and AMS/ACSM-PMF first, as presented in Fig. 1. The results from all 4 methods for samples obtained on identical days will be discussed later (Table 2).

AMS/ACSM-PMF apportioned OC into traffic (HOC), coal combustion (CCOC), biomass burning (BBOC), cooking (COC) and SOC (*i.e.*, OOC). In addition to these sources, the CMB model can also differentiate gasoline and diesel emissions in the traffic source category. Vegetative detritus is a minor source of OC in PG which was only resolved by the CMB model. PMF of filter-based data resulted in 7 factors: coal combustion, traffic, oil combustion, biomass burning, secondary inorganic ions, road dust and soil dust, in which road and soil dust were combined into a single dust source.

The reconstructed OC (sum of OC in each source category) in the middle of the pie charts (Fig. 1) for CMB was the same as the measured OC; the differences in concentration level between the reconstructed OC and the observed OC in Table 1 were because a small number of samples were not included in the CMB modelling due to insufficient speciation data. The reconstructed OC masses in NR-PM_1 for

Open Access Article. Published on 23 2020. Downloaded on 09-10-2024 6:25:25.
This article is licensed under a Creative Commons Attribution 3.0 Unported Licence.

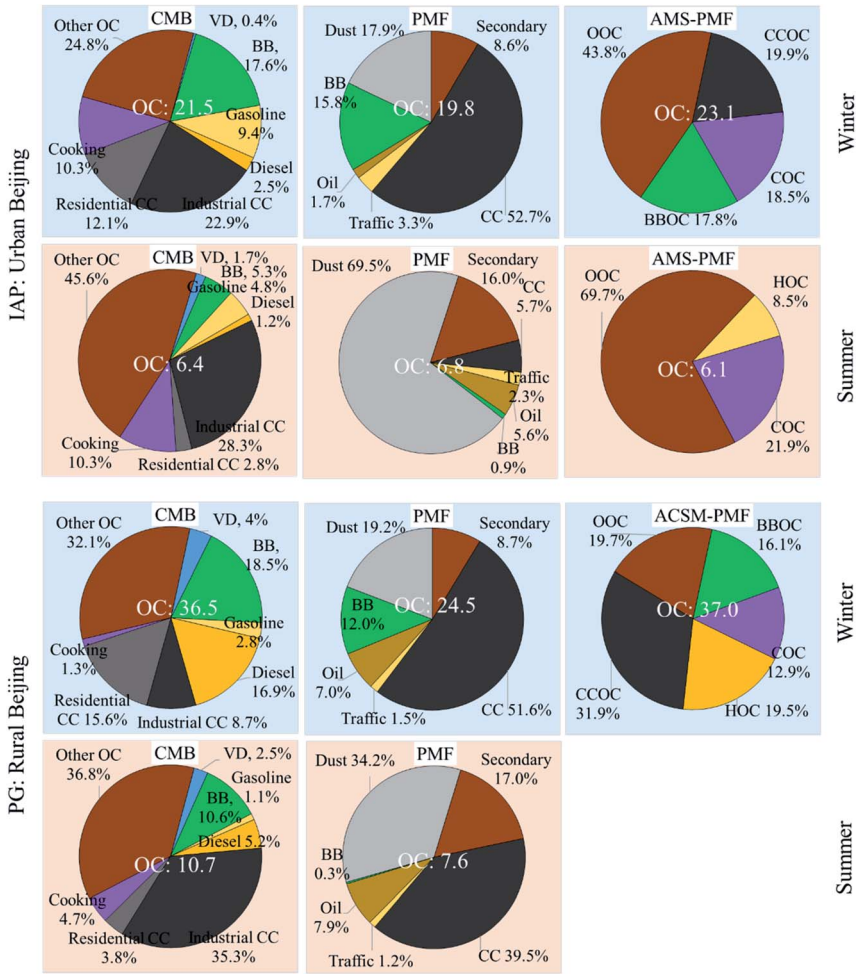

Fig. 1 Source contributions to OC in winter (blue-shaded) and summer (pink-shaded) at the IAP and PG sites by CMB, PMF and AMS/ACSM-PMF (note: the reconstructed OC in the middle of the pie chart is the sum of the OC from each source; VD: vegetative detritus; BB: biomass burning; CC: coal combustion; OOC: oxidized OC; CCOC: coal combustion OC; BBOC: biomass burning OC; COC: cooking OC; HOC: hydrocarbon-like (traffic) OC).

the AMS/ACSM-PMF data were comparable with those in $PM_{2.5}$ for CMB. This agrees in general with Guo (2016)[43] that OC fractions in fine particles are mostly concentrated in particles <1 μm; in addition, there are some uncertainties in converting organic aerosols (OAs) into OC in the AMS/ACSM-PMF results using OA/OC ratios from the literature (ESI†). The reconstructed OC for PMF was mostly lower than that for the other methods, which is due to the inability of PMF to model heavily polluted events. In the CMB source apportionment results, seven primary sources explained 56.1–75.7% of OC at IAP and PG in both seasons. The unexplained OC (other OC) was considered to be mostly SOC based on the good correlation (R^2: 0.6–0.7; slope: 1.0 ± 0.2) between the "other OC" and the SOC estimated based on OC/EC ratios.[36] PMF did not resolve SOC but yielded a factor for secondary inorganics, which may contain some secondary OC.

Open Access Article. Published on 23 2020. Downloaded on 09-10-2024 6:25:25.
This article is licensed under a Creative Commons Attribution 3.0 Unported Licence.

Table 2 Comparison of OC source apportionment results (μg m^{-3}) obtained using different methods in winter and summer for the IAP and PG sites in Beijing (only for samples where ^{14}C was analysed)

		IAP winter ($n = 7$)				IAP summer ($n = 6$)			
		CMB	EG method	AMS/ACSM -PMF	PMF	CMB	EG method	AMS/ACSM -PMF	PMF
OC		26.8 ± 14.2	26.8 ± 14.2	29.0 ± 18.1	26.3 ± 13.8	8.3 ± 3.2	8.3 ± 3.2	7.5 ± 3.4	8.7 ± 3.3
POC	Traffic (POC_{tra})	3.3 ± 2.8	2.1 ± 1.3[b]	—	0.6 ± 0.4	0.5 ± 0.2	0.5 ± 0.2	0.5 ± 0.1	0.3 ± 0.3
	Coal combustion (POC_{cc})	8.7 ± 6.0	8.4 ± 4.9[c]	5.2 ± 3.3	16.6 ± 9.9	2.4 ± 0.5	1.8 ± 0.6	—	0.8 ± 1.1
	Oil combustion	—[a]	—	—	0.1 ± 0.1	—	—	—	0.2 ± 0.1
	Sum (POC_f)	**12.0 ± 6.5**	**10.5 ± 6.2**	**5.2 ± 3.3**	**17.3 ± 10.1**	**2.8 ± 0.5**	**2.3 ± 0.8**	**0.5 ± 0.1**	**1.3 ± 1.2**
	Vegetative detritus	0.1 ± 0.1	—	—	—	0.2 ± 0.1	—	—	—
	Biomass burning (POC_{bb})	4.4 ± 2.5	2.7 ± 1.3	5.8 ± 4.7	3.3 ± 2.3	0.6 ± 0.8	0.6 ± 0.7	—	0.1 ± 0.1
	Cooking (POC_{ck})	2.8 ± 3.1	1.1 ± 0.7	4.1 ± 2.0	—	0.6 ± 0.3	1.1 ± 0.4	1.3 ± 0.2	—
	Dust	—	—	—	3.1 ± 2.6	—	—	—	5.2 ± 2.0
	Sum (POC_{nf})	**7.3 ± 4.9**	**3.8 ± 1.9**	**9.9 ± 6.5**	**6.4 ± 4.0**	**1.5 ± 1.1**	**1.8 ± 0.5**	**1.3 ± 0.2**	**5.3 ± 2.0**
SOC	SOC_f	—	7.7 ± 4.2	—	—	—	2.0 ± 0.9	—	—
	SOC_{nf}	—	4.8 ± 2.9	—	—	—	2.2 ± 2.1	—	—
	Sum	**7.4 ± 5.7**	**12.5 ± 6.5**	**13.9 ± 8.9**	**2.5 ± 2.2**	**4.0 ± 2.2**	**4.3 ± 2.5**	**5.6 ± 3.4**	**2.2 ± 1.8**
		PG winter ($n = 7$)				PG summer ($n = 5$)			
		CMB	EG method	AMS/ACSM -PMF	PMF	CMB	EG method	AMS/ACSM -PMF	PMF
OC		48.9 ± 27.3	48.9 ± 27.3	48.3 ± 26.1	32.1 ± 17.4	11.5 ± 4.9	11.5 ± 4.9	N.D.[d]	11.0 ± 3.4
POC	Traffic (POC_{tra})	10.0 ± 6.0	2.7 ± 1.3	9.6 ± 5.4	0.4 ± 0.3	0.8 ± 0.3	1.0 ± 0.6	N.D.	0.1 ± 0.1
	Coal combustion (POC_{cc})	11.1 ± 5.4	13.3 ± 6.5	14.9 ± 7.9	17.5 ± 13.5	4.6 ± 2.5	2.3 ± 1.3	N.D.	4.3 ± 2.1
	Oil combustion	—	—	—	2.0 ± 2.3	—	—	N.D.	1.0 ± 0.5
	Sum (POC_f)	**21.0 ± 10.8**	**16.0 ± 7.8**	**24.5 ± 13.3**	**19.9 ± 12.1**	**5.4 ± 2.5**	**3.3 ± 1.9**	**N.D.**	**5.5 ± 2.2**
	Vegetative detritus	2.5 ± 4.1	—	—	—	0.3 ± 0.3	—	N.D.	—

Open Access Article. Published on 23 2020. Downloaded on 09-10-2024 6:25:25.
This article is licensed under a Creative Commons Attribution 3.0 Unported Licence.

Table 2 (*Contd.*)

		PG winter ($n = 7$)				PG summer ($n = 5$)			
		CMB	EG method	AMS/ACSM -PMF	PMF	CMB	EG method	AMS/ACSM -PMF	PMF
	Biomass burning (POC_{bb})	9.2 ± 5.5	4.8 ± 2.4	8.0 ± 5.8	4.2 ± 3.2	1.2 ± 0.7	2.0 ± 0.8	N.D.	0.0 ± 0.0
	Cooking (POC_{ck})	0.3 ± 0.3	5.8 ± 3.6	6.0 ± 2.0	—	0.6 ± 0.4	0.9 ± 0.4	N.D.	—
	Dust	—	—	—	3.5 ± 4.0	—	—	N.D.	3.5 ± 0.8
	Sum (POC_{nf})	**12.0 ± 9.0**	**10.6 ± 5.7**	**14.0 ± 7.7**	**7.7 ± 6.4**	**2.0 ± 1.4**	**2.9 ± 0.6**	**N.D.**	**3.5 ± 0.8**
SOC	SOC_f	—	13.3 ± 10.4	—	—	—	2.1 ± 1.5	N.D.	—
	SOC_{nf}	—	9.1 ± 9.0	—	—	—	3.1 ± 3.1	N.D.	—
	Sum	**15.9 ± 9.6**	**22.4 ± 17.4**	**9.8 ± 5.4**	**4.6 ± 5.1**	**4.1 ± 2.5**	**5.2 ± 3.3**	**N.D.**	**2.0 ± 1.4**

[a] "—" means the method could not resolve the corresponding source. [b] Maximum value for traffic related POC (POC_{tra}), which is calculated by multiplying EC_f by the OC/EC ratio for primary traffic emissions (0.85 ± 0.16) in China,[44] assuming that EC_f only originates from traffic emissions. [c] Minimum value for coal combustion related POC, which is calculated by subtracting the maximum POC_{tra} from POC_f. [d] "N.D." means no data available.

This journal is © The Royal Society of Chemistry 2021

Open Access Article. Published on 23 2020. Downloaded on 09-10-2024 6:25:25.
This article is licensed under a Creative Commons Attribution 3.0 Unported Licence.

In winter, fossil fuel (the sum of diesel, gasoline, industrial and residential coal combustion) related POC_f contributed 46.9% and 44.0% of OC at IAP and PG, respectively, according to the CMB results. For PMF, the fossil fuel sources (the sum of traffic, oil and coal combustion) contributed 57.7% and 60.1% of OC at IAP and PG, respectively. The higher percentages for PMF may be because PMF did not separate well the POC and SOC. HOC was not resolved at the IAP site by AMS-PMF, hence, fossil fuel related POC (CCOC) contributed only 19.9% of OC, while its contribution (the sum of CCOC and HOC) at the PG site (51.4%) was similar to that for CMB and PMF. Coal combustion contributed 20–35% of OC for CMB and AMS/ACSM-PMF at both sites in winter. The much higher contribution (around 50%) for PMF could be the result of unseparated POC and SOC. For CMB, traffic emissions (diesel and gasoline) contributed 11.9% and 19.7% at IAP and PG, respectively, which are close to the values for AMS/ACSM-PMF (HOC), but much higher than the values for PMF. Biomass burning was resolved by all methods; it contributed from 15.8% to 17.8% of reconstructed OC at IAP, and 12.0% to 18.5% of reconstructed OC at PG for CMB, PMF and AMS/ACSM-PMF. Cooking was not identified in the PMF factors and its contributions to OC resolved by CMB (10.3% and 1.3% for IAP and PG, respectively) were different to those resolved by AMS/ACSM-PMF (18.5% and 12.9% for IAP and PG, respectively).

In summer, the estimated contributions of primary sources of OC varied significantly for the three methods. Dust related OC was a dominant contributor in the PMF results, which is doubtful. The dust factor was probably associated with SOC as this factor was observed with the second highest concentrations of nitrate and sulfate, after the factor of secondary inorganics. The contribution of fossil fuel sources to OC is similar for the CMB (45.4%) and PMF (48.6%) analyses at PG. Other sources such as cooking and biomass burning also varied for the different methods.

^{14}C was determined in 25 samples. For consistency, the source apportionment results from CMB, PMF and AMS/ACSM-PMF for the 25 samples were singled out for further comparison (Table 2). More details of the source apportionment results from the 4 methods can be found in Tables S2–S5.† The EG method was not able to quantify POC from traffic and coal combustion, but a maximum value for traffic related POC (POC_{tra}) can be estimated by multiplying EC_f by the OC/EC ratio for primary traffic emissions (0.85 ± 0.16) in China,[44] assuming that EC_f only originates from traffic emissions. A minimum value for coal combustion related POC can be subsequently calculated by subtracting the maximum POC_{tra} from POC_f.

In general, the average reconstructed OC concentrations were comparable for the four methods on identical days, except for PMF at PG during winter. The POC_f estimated by CMB was on average 1.1, 1.3, 1.2 and 1.6 times higher than the EG-based results for IAP and PG in winter and summer, respectively. For the EG method, POC_f was estimated as EC_f multiplied by the ratio of $OC/EC_{f,min}$. The significantly lower POC_f estimated by the EG method at PG in summer is due to the relatively low $OC/EC_{f,min}$ ratios used for the calculation. The much lower estimates of POC_f at IAP by AMS/ACSM-PMF were due to the failure of AMS/ACSM-PMF to resolve either HOC or CCOC. When HOC and CCOC were both resolved at PG during winter, the POC_f estimated by AMS/ACSM-PMF was comparable with that estimated by CMB. Coal combustion (POC_{cc}) differed for the 4 methods

Open Access Article. Published on 23 2020. Downloaded on 09-10-2024 6:25:25.
This article is licensed under a Creative Commons Attribution 3.0 Unported Licence.

except for the comparable results for the EG method and CMB at IAP and PG during winter. The traffic related POC (POC_{tra}) results were consistent for CMB, EG and AMS/ACSM-PMF in summer, but the EG method provided different results in winter. The maximum POC_{tra} for the EG method was much lower than that for CMB and AMS/ACSM-PMF. This could be due to the use of an unrepresentative OC/EC ratio for primary traffic emissions (0.85 ± 0.16) in China,[44] which may be seasonally variable. This ratio should be higher in winter than in summer because faster catalyst and engine warm-up times and more volatilization of semi-volatile organic compounds in summer will cause a decrease in the OC/EC ratio in traffic emissions.[45] Hence, POC_{tra} in winter may be underestimated by the EG method. AMS/ACSM-PMF only resolved POC_{bb} in the wintertime and the results were generally similar to the CMB results, while the values obtained by the EG method and PMF were much lower. In the summertime, the POC_{bb} contributions estimated by the EG method and CMB were very close, but that estimated by PMF was extremely low. A discrepancy was also found for cooking (POC_{ck}), where the estimated contributions were only comparable for the EG method and AMS/ACSM-PMF at PG during winter and IAP during summer. The sum of POC_{bb} and POC_{ck} in AMS/ACSM-PMF at IAP during winter was 9.9 ± 6.5 μg m^{-3}, which was higher than the OC_{nf} (POC_{bb} + POC_{ck} + SOC_{nf}; 8.6 ± 4.7 μg m^{-3}) measured through ^{14}C analysis, suggesting that the sum of POC_{bb} and POC_{ck} in AMS/ACSM-PMF was overestimated at IAP during winter. The overestimation of POC_{ck} could be due to the use of a relatively low OA/OC ratio for the cooking source or a low RIE for cooking OAs (1.4) in AMS. The actual RIE could be higher, for example 1.56–3.06 as reported in another study.[46]

The results from the four methods are further compared through correlation analysis and discussed in Section 3.3. Due to the absence of ACSM-PMF data at PG during summer, the comparisons were conducted on the 20 samples for which all methods gave results. In addition, the OC source apportionment results from the four methods for haze samples ($n = 11$) and non-haze samples ($n = 9$) are

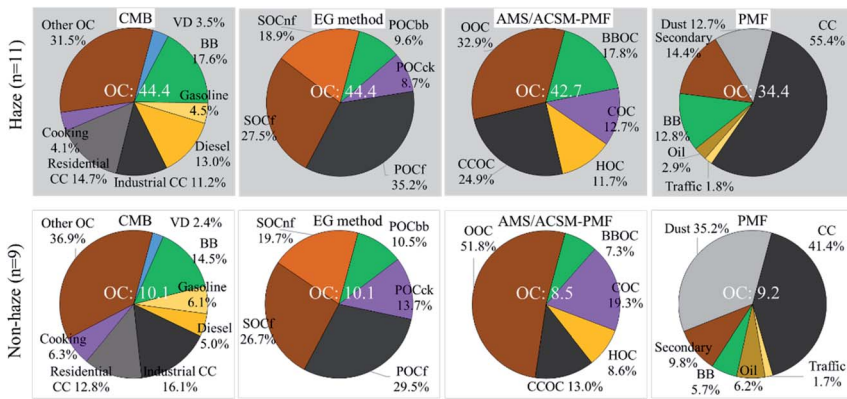

Fig. 2 Source contributions to OC on haze (grey) and non-haze (white) days in Beijing estimated by CMB, the EG method, PMF and AMS/ACSM-PMF (note: the OC in the middle of the pie chart is the reconstructed OC, which is the sum of the OC from each source; VD: vegetative detritus; BB: biomass burning; CC: coal combustion; OOC: oxidized OC; CCOC: coal combustion OC; BBOC: biomass burning OC; COC: cooking OC; HOC: hydrocarbon-like (traffic) OC).

Open Access Article. Published on 23 2020. Downloaded on 09-10-2024 6:25:25.
This article is licensed under a Creative Commons Attribution 3.0 Unported Licence.

compared in Fig. 2. On haze days, CMB and AMS/ACSM-PMF were consistent in apportioning OC into POC_f, POC_{nf} and SOC. The POC_f estimated by the EG method was consistent with that estimated by CMB and AMS/ACSM-PMF, but SOC was much higher for the EG method than the others, and POC_{nf} was lower for the EG method than for CMB and AMS/ACSM-PMF. Coal combustion and biomass burning OC were also comparable in the CMB and AMS/ACSM-PMF results. Cooking was more difficult to resolve as mentioned above. The reconstructed OC (34.4 μg m^{-3}) for PMF was much lower than those (42.7–44.4 μg m^{-3}) for the other methods, indicating that PMF had problems resolving OC sources in haze samples. The PMF factors were also less comparable with the sources estimated by the other methods, except for BB. On non-haze days, the factors in the four methods were less comparable, suggesting the difficulty of OC source apportionment for non-haze samples, especially by PMF. The dust factor in PMF could be associated with SOC based on the comparison with the other methods.

3.3 Correlation analysis

An orthogonal regression analysis was conducted on the results from CMB, the EG method and AMS/ACSM-PMF for identical days. The PMF results are not compared here because the method did not separate POC and SOC and its results differed the most from those of the other methods.

3.3.1 Primary OC from fossil fuel combustion (POC_f). For the EG method, POC_f was calculated by multiplying EC_f by the estimated minimum $(OC/EC)_f$ ratios at both sites during winter and summer. POC_f was calculated from the CMB results as the sum of gasoline, diesel, industrial and residential coal combustion, while for AMS/ACSM-PMF, POC_f was the sum of HOC and CCOC. The orthogonal regression results for POC_f estimated by the three methods are plotted in Fig. 3.

In the comparison of POC_f estimated by the three methods, strong correlations ($r^2 > 0.6$) were found between them with slopes ranging between 0.78–1.26. The CMB-resolved POC_f was found to be significantly correlated ($r^2 > 0.8$) with those from the other two methods (Fig. 3). When excluding the two extreme datapoints (POC_f-AMS/ACSM-PMF > 30 μg m^{-3}), the POC_f estimated by the EG method and AMS/ACSM-PMF were also highly correlated with r^2 of 0.77 and slope of 0.82. This probably suggests a bigger uncertainty for AMS/ACSM-PMF in estimating POC_f at high concentrations. For the coal combustion POC estimated by CMB and AMS/ACSM-PMF, the slope was close to unity with r^2 of 0.45 (Fig. S2(a)†). For POC_{tra} estimated by the two methods, the concentrations were generally consistent

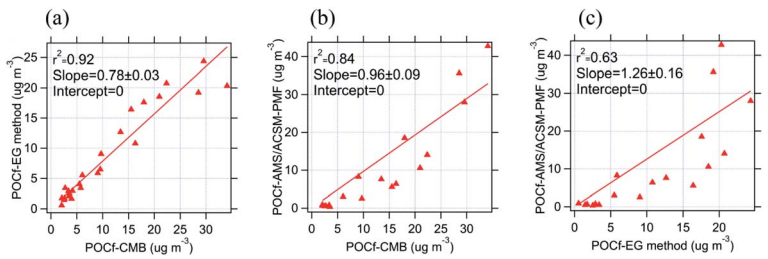

Fig. 3 Correlations of POC_f estimated by different methods: (a) extended Gelencsér (EG) method *vs.* CMB; (b) AMS/ACSM-PMF *vs.* CMB; (c) AMS/ACSM-PMF *vs.* EG method.

Open Access Article. Published on 23 2020. Downloaded on 09-10-2024 6:25:25.
This article is licensed under a Creative Commons Attribution 3.0 Unported Licence.

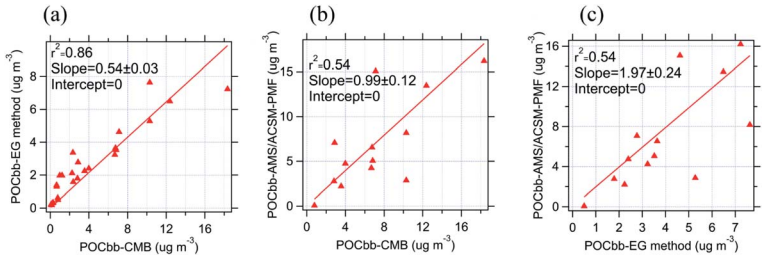

Fig. 4 Correlations of POC_{bb} estimated by different methods: (a) extended Gelencsér (EG) method *vs.* CMB; (b) AMS/ACSM-PMF *vs.* CMB; (c) AMS/ACSM-PMF *vs.* EG method.

(Table 2) and well correlated with r^2 of 0.91 and slope of 0.87 (Fig. S2(b)†). But there is no correlation between the two methods at IAP during summer (Fig. S11(d)†). It is challenging to apportion POC_{tra} when the concentrations are low.

3.3.2 Primary OC from biomass burning (POC_{bb}). The correlations of POC_{bb} estimated by the three methods are shown in Fig. 4. The POC_{bb} estimated by CMB was mainly characterized by high concentrations of anhydrous sugars like levoglucosan, while POC_{bb} in AMS/ACSM-PMF was identified by prominent peaks at m/z 60 and 73, which are typical fragments of anhydrous sugars like levoglucosan.[47] The POC_{bb} results from both methods were comparable with a slope of 0.99 and r^2 of 0.54. POC_{bb} was estimated by the EG method using the OC/levoglucosan and EC/OC ratios (ESI†). The EG results correlated well with those from CMB ($r^2 = 0.86$), but the absolute concentration of POC_{bb} estimated by the EG method was only approximately 50% of that estimated by CMB in winter at IAP (4.4 ± 2.5 μg m^{-3}) and PG (9.2 ± 5.5 μg m^{-3}) (Table 2). In summer, when the POC_{bb} contribution was significantly lower than that in winter, the POC_{bb} estimated by the EG method was comparable with that estimated by CMB at IAP, and much higher than that estimated by CMB at PG. In this study, different OC/levoglucosan and EC/OC ratios were applied when calculating POC_{bb} by the EG method. The ratios were obtained from softwood for the winter and summer campaign and maize straws in winter but from softwood and wheat straws in summer after analysing the corresponding relationship of levoglucosan with mannosan and galactosan. Besides, levoglucosan was reported to be less stable in summer due to a higher degradation rate, especially under high relative humidity conditions.[48] Hence, the EG method may introduce uncertainties in the POC_{bb} concentrations due to various factors, for example uncertainty in the OC/levoglucosan ratios. The correlation results for the three methods at IAP and PG during winter and summer are provided in Fig. S3.† Good correlations were found between the EG method and the other two methods at both sites, but the absolute POC_{bb} concentrations estimated by the EG method are different to those from the other methods.

3.3.3 Primary OC from cooking (POC_{ck}). The CMB results for POC_{ck} were mainly characterized by high concentrations of palmitic and stearic acids, which are the predominant compounds in cooking emissions.[49] The POC_{ck} estimated by AMS/ACSM-PMF was characterized by high peaks for the fragment ions $C_3H_3O^+$, $C_4H_7^+$, $C_3H_5O^+$, and $C_4H_9^+$ at m/z 55 and 57 in the mass spectrum.[50] No correlation between the three methods was observed for POC_{ck}, as shown in Fig. 5. POC_{ck} was estimated by the EG method as the difference between POC_{nf} and POC_{bb}, and

Open Access Article. Published on 23 2020. Downloaded on 09-10-2024 6:25:25.
This article is licensed under a Creative Commons Attribution 3.0 Unported Licence.

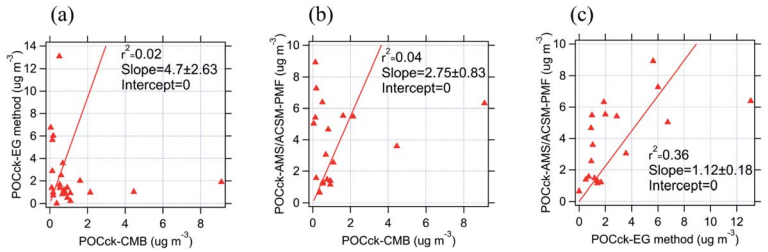

Fig. 5 Correlations of POC_{ck} estimated by different methods: (a) extended Gelencsér (EG) method *vs.* CMB; (b) AMS/ACSM-PMF *vs.* CMB; (c) AMS/ACSM-PMF *vs.* EG method.

other biogenic POC was neglected. Hence, POC_{ck} could be overestimated by the EG method. AMS/ACSM-PMF is unable to separate traffic and cooking emissions perfectly.[17–19] Elser *et al.*[51] proposed the use of a multilinear engine (ME-2) controlled *via* a source finder (SoFi) to improve the source apportionment results obtained by PMF of AMS data. Abdullahi *et al.*[52] applied CMB for the source apportionment of atmospheric aerosols using the chemical profiles of molecular markers such as alkanes, PAHs, acids, and sterols from four different styles of cooking: Indian, Chinese, African and Western cooking. Their results showed very low sensitivity of CMB to the different cooking profiles applied, despite the difference in the source profiles. This may explain the less satisfactory correlation of POC_{ck} estimated by the 3 methods. Cooking was also reported as one of the most difficult sources to characterize in receptor modelling.[46] The correlation of POC_{ck} estimated using all three methods at IAP and PG during winter and summer was also investigated (Fig. S4†). No obvious correlation was observed, except at IAP in winter for the EG method and AMS-PMF, suggesting a large uncertainty in estimating POC_{ck}.

3.3.4 Primary OC from non-fossil sources (POC_{nf}). The correlations of POC_{nf} estimated by the three methods were also investigated (Fig. S5†). In the CMB results, POC_{nf} is the sum of vegetative detritus, biomass burning and cooking. For the EG method and AMS/ACSM-PMF, POC_{nf} is the sum of POC_{bb} and POC_{ck}. The correlation between CMB and AMS/ACSM-PMF was good with r^2 of 0.83 and slope of 1.1. But the correlation between the EG method and the other two methods was not very good with r^2 of 0.50–0.55 and slopes of 0.73–1.56. Uncertainties within the apportionments of POC_{bb} and POC_{ck} by the three methods make it difficult to quantify total non-fossil POC.

3.3.5 Secondary OC from all sources (SOC). The SOC estimated by AMS/ACSM-PMF was poorly correlated with that estimated by the other two methods (Fig. 6). However, the SOC estimated by the EG method and the other OC estimated by CMB were better correlated with r^2 of 0.72 and slope of 1.54. The correlation results for SOC estimated using all three methods at IAP and PG during winter and summer are provided in Fig. S6.† The SOC concentrations for the three methods correlated well with each other ($r^2 > 0.8$) in summer at IAP and PG, with slopes ranging between 1.09 and 1.44. In winter, AMS/ACSM-PMF generally correlated well with the other two methods (Fig. S6†), but the absolute concentrations varied appreciably.

Open Access Article. Published on 23 2020. Downloaded on 09-10-2024 6:25:25.
This article is licensed under a Creative Commons Attribution 3.0 Unported Licence.

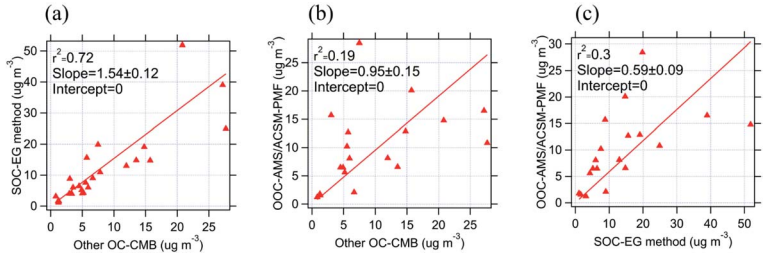

Fig. 6 Correlations of SOC estimated by different methods: (a) extended Gelencsér (EG) method *vs.* CMB; (b) AMS/ACSM-PMF *vs.* CMB; (c) AMS/ACSM-PMF *vs.* EG method.

3.4 Source apportionment of $PM_{2.5}$

The $PM_{2.5}$ source apportionment results from PMF, CMB and AMS/ACSM-PMF were compared for samples collected on identical days (Table 3). It should be noted that PMF modelling was conducted based on filter-based data from 133 samples at both sites during winter and summer (Table S4†) but a comparison was only made for the dates when data was available for all methods. To reconstruct $PM_{2.5}$ using the OC source apportionment results obtained by CMB, the source contributions were calculated using the source-specific OC concentration multiplied by the $OC/PM_{2.5}$ ratio in the corresponding source profile; more details can be found elsewhere.[36] In addition, dust and SNA (sum of measured sulfate, nitrate and ammonium) were also added; dust (geological minerals) was calculated by eqn (1) below,[53] and for AMS/ACSM-PMF, SNA is the non-refractory sulfate, nitrate and ammonium in NR-$PM_{1.0}$.

$$\text{Geological minerals} = 2.2\text{Al} + 2.49\text{Si} + 1.63\text{Ca} + 1.94\text{Ti} + 2.42\text{Fe} \quad (1)$$

As shown in Table 3, the measured concentrations of SNA at IAP were higher than those of the corresponding factor in PMF, but they were comparable at PG. The SNA concentration in the AMS data was much higher than the measured SNA concentration during winter, but lower than that in summer at IAP. Differences were also found between online ACSM and filter-based SNA concentrations in another study.[54] Possible reasons could be the uncertainties of SNA in ACSM analysis,[55] and the evaporation of ammonium nitrate and the difficulties in separating organosulfate from sulfate in AMS.[56] The lower average SNA concentration in PMF is probably due to the contribution of the secondary inorganics factor being zero in some samples, as computed by PMF. The dust concentration in PMF was around 2–3 times that estimated in the CMB results, suggesting that one of the PMF dust factors is misassigned.

For organics, PMF was unable to resolve either cooking or secondary sources. For coal combustion, the estimates were comparable for both CMB and PMF results in winter. But in summer, the concentration for CMB was higher than that in the PMF results. It is difficult for PMF to resolve different factors (both offline and online) when the concentrations are relatively low. However, CMB appears to be more sensitive in resolving different sources in low concentration PM samples. As the coal combustion factor was resolved by all methods at both sites during

Open Access Article. Published on 23 2020. Downloaded on 09-10-2024 6:25:25.
This article is licensed under a Creative Commons Attribution 3.0 Unported Licence.

Table 3 Comparison of $PM_{2.5}$ source apportionment results (μg m^{-3}) obtained using different methods in winter and summer at the IAP and PG sites in Beijing

	IAP winter ($n = 24$)			IAP summer ($n = 30$)		
	CMB	AMS/ACSM-PMF	PMF	CMB	AMS/ACSM-PMF	PMF
SNA	30.4 ± 21.9	44.5 ± 35.4	18.6 ± 18.5	18.1 ± 11	11.9 ± 7.2	11.7 ± 12.1
Dust	5.4 ± 3.4	—[a]	8.5 ± 5.9	3.5 ± 1.9	—	12.1 ± 5.0
Coal combustion	18.6 ± 12.1	6.5 ± 4.5	17.4 ± 15.0	4.5 ± 1.8	0.0 ± 0.0	0.6 ± 1.0
Traffic	6.1 ± 5.3	0.0 ± 0.0[b]	7.1 ± 6.7	0.8 ± 0.4	0.7 ± 0.4	1.8 ± 1.8
Biomass burning	8.8 ± 6.6	6.8 ± 5.9	30.4 ± 20.4	0.8 ± 1	0.0 ± 0.0	0.5 ± 0.6
Cooking	3.1 ± 2.8	6.1 ± 4.2	—	1.0 ± 0.6	1.8 ± 1	—
Oil combustion	—	—	1.3 ± 1.5	—	—	1.6 ± 1.9
Secondary OM	13.1 ± 11.9	19.0 ± 13.3	—	6.2 ± 3.3	7.6 ± 3.7	—
Sum	**85.6 ± 51.3**	**90.1 ± 64.2**	**83.2 ± 49.4**	**35 ± 15.9**	**22.2 ± 10.3**	**28.3 ± 14.8**
Gravimetric $PM_{2.5}$	**98.2 ± 67.5**			**30.4 ± 15.5**		
	PG winter ($n = 11$)			PG summer ($n = 6$)		
	CMB	AMS/ACSM-PMF	PMF	CMB	AMS/ACSM-PMF	PMF
SNA	38.5 ± 40.2	N.D.[c]	33.8 ± 45.6	21.8 ± 15.5	N.D.	17.2 ± 15.3
Dust	3.2 ± 2.2	—	7.9 ± 8.5	3.2 ± 1.3	—	7.7 ± 2.6
Coal combustion	24.9 ± 12.3	15.9 ± 11.4	21.1 ± 19	9.8 ± 5.9	N.D.	6.6 ± 2.8
Traffic	16.3 ± 11.6	9.4 ± 7.3	3.8 ± 3.5	1.2 ± 0.6	N.D.	1.2 ± 1.4
Biomass burning	19.4 ± 13	9.4 ± 8.7	31.7 ± 27.5	2.7 ± 1.5	N.D.	0.1 ± 0.3

Open Access Article. Published on 23 2020. Downloaded on 09-10-2024 6:25:25.
This article is licensed under a Creative Commons Attribution 3.0 Unported Licence.

Table 3 (*Contd.*)

	PG winter ($n = 11$)			PG summer ($n = 6$)		
	CMB	AMS/ACSM-PMF	PMF	CMB	AMS/ACSM-PMF	PMF
Cooking	0.8 ± 0.7	6.6 ± 3.6	—	0.7 ± 0.6	N.D.	—
Oil combustion	—	—	7.4 ± 7.9	—	—	3.9 ± 2.2
Secondary OM	31.3 ± 22.8	12.9 ± 10.3	—	8.6 ± 5.0	N.D.	—
Sum[d]	**138.0 ± 99.4**	—	**105.8 ± 87.7**	**48.6 ± 23.9**	**N.D.**	**36.6 ± 20.4**
Gravimetric $PM_{2.5}$	**131.9 ± 107.6**			**38.0 ± 22.0**		

[a] "—" means the method could not resolve the corresponding source. [b] The source contribution is marked as "0.0 ± 0.0" when it is too low to be identified as a single factor in AMS/ACSM-PMF. [c] "N.D." means no data available. [d] Sum is the sum of all sources listed in the table and additional sources: for CMB, sum also includes vegetative detritus; for AMS/ACSM-PMF, it also includes NR-Cl^-.

This journal is © The Royal Society of Chemistry 2021

Open Access Article. Published on 23 2020. Downloaded on 09-10-2024 6:25:25.
This article is licensed under a Creative Commons Attribution 3.0 Unported Licence.

winter, the time series and correlations at IAP and PG are provided in Fig. S7 and S8,† respectively. Generally good correlation ($r^2 > 0.7$) was only found between CMB and AMS/ACSM-PMF at both sites, but the concentrations were somewhat different.

The time series of biomass burning aerosols at both sites estimated by all 3 methods followed a similar trend (Fig. S9 and S10†). Moderately good correlations of the 3 methods were found at PG, but the concentrations varied. Biomass burning is a significant factor in PMF, which resulted in over 30 μg m^{-3} of BB-related $PM_{2.5}$ in winter at both sites. This is much higher than the BB aerosol concentrations estimated by CMB and AMS/ACSM-PMF. A comparative analysis of applications of PMF to multi-constituent chemical datasets from Beijing has demonstrated the inconsistency of their findings and the problematic nature of the application of this method to Beijing aerosols,[41] consistent with the findings of this study. In summer, the BB-related $PM_{2.5}$ concentrations estimated by CMB were 0.8 and 2.7 μg m^{-3} at IAP and PG, respectively. However, those estimated by PMF were only 0.5 and 0.1 μg m^{-3} at IAP and PG, respectively. PG is a rural site, where BB is used for cooking and heating. This is shown in the results from both the ^{14}C/EG method and CMB. Hence, PMF probably did not successfully resolve BB emissions.

The average concentrations of traffic related particles were generally low and comparable for the different methods in summer, but with no correlation of the time series and concentrations (Fig. S11†). In winter, the concentrations of traffic particles are comparable for CMB (6.1 ± 5.3 μg m^{-3}) and PMF (7.1 ± 6.7 μg m^{-3}) at IAP but no obvious correlation is observed (Fig. S12†); those estimated by CMB (16.3 ± 11.6 μg m^{-3}) and ACSM-PMF (9.4 ± 7.3 μg m^{-3}) at PG were much higher than that estimated by PMF (3.8 ± 3.5 μg m^{-3}), but the time series are well correlated (Fig. S13†).

Cooking emissions were only resolved by CMB and AMS/ACSM-PMF. At the IAP site, the cooking OA (COA) concentrations estimated by CMB are about half those estimated by AMS-PMF during both seasons, which is consistent with other studies which reported that COA was overestimated around 2-fold by AMS-PMF.[4,46] The COA concentration at PG was much higher in the ACSM-PMF results (6.6 ± 3.6 μg m^{-3}) than for CMB (0.8 ± 0.7 μg m^{-3}), suggesting other influences on one or the other method.

Overall, the CMB source apportionment results appear more representative of reality based on the intercomparison and correlation analysis. From the CMB modelling results, the major sources of $PM_{2.5}$ in Beijing were secondary inorganic ions, secondary organic aerosols, primary coal combustion and biomass burning emissions. The relative abundance of source contributions (%) in the CMB results at IAP and PG during haze and non-haze days was also investigated (Table S6†). SNA increased significantly during haze days, especially on the haze day (27th May 2017) in summer. This is consistent with secondary inorganic aerosol formation making a major contribution to haze formation in Beijing. Liu *et al.* (2019)[57] applied PMF for $PM_{2.5}$ source apportionment of online data recorded in urban Beijing (Peking University, PKU) with 1 h time resolution during the same winter campaign and resolved 6 sources including dust, coal, industry, traffic, biomass and secondary sources. The contribution from combined coal and industry sources to $PM_{2.5}$ for PMF at PKU was comparable with that from combined industrial and residential coal combustion for CMB at IAP (Table S6†) during haze

Open Access Article. Published on 23 2020. Downloaded on 09-10-2024 6:25:25.
This article is licensed under a Creative Commons Attribution 3.0 Unported Licence.

(22–24%) and non-haze days (20–21%). The contributions from biomass burning, dust and traffic emissions to $PM_{2.5}$ were higher on non-haze days in both studies. But the percentages of biomass burning and traffic were generally much higher for PMF-PKU than CMB, especially on non-haze days. While secondary particles (SNA + secondary OM) during haze and non-haze days were higher for CMB (52% and 45%) than for PMF-PKU (44% and 21%). This is probably because the secondary organic sources were not very well separated in PMF as mentioned earlier.

4. Summary

The ^{14}C/extended Gelencsér (EG) method, PMF, CMB and AMS/ACSM-PMF were used for the source apportionment of OC, EC and $PM_{2.5}$ at urban and rural sites in Beijing during winter and summer. The results from these methods were intercompared and evaluated through correlation analysis. The results of the OC source apportionment intercomparison are summarized here:

(1) The reconstructed OC from all apportioned sources was comparable for CMB, the EG method and AMS/ACSM-PMF, but lower for PMF, which is due to the inability of PMF to model heavily polluted events and separate POC and SOC.

(2) CMB, the EG method and AMS/ACSM-PMF provide a consistent apportionment of POC_f in haze samples. CMB and the EG method are consistent in separating OC into POC_f, POC_{nf} and SOC in non-haze samples, but the AMS/ACSM-PMF and PMF methods are not.

(3) For fossil fuel sources, a strong correlation was found between CMB and both the EG method and AMS/ACSM-PMF for POC_f. Coal combustion POC (POC_{cc}) and traffic POC (POC_{tra}) were also correlated for CMB and AMS/ACSM-PMF, with slopes close to 1.

(4) For non-fossil fuel sources, the correlation of POC_{nf} estimated by CMB and AMS/ACSM-PMF was good with r^2 of 0.83 and a slope of 1.1, while the correlation of the POC_{nf} estimated by the EG method with that estimated by CMB and AMS/ACSM-PMF was not very good. The POC_{bb} concentrations provided by CMB and AMS/ACSM-PMF were more comparable. The POC_{ck} concentrations were less correlated for the three methods, suggesting large uncertainty in estimating POC_{ck}.

Receptor modelling of $PM_{2.5}$ in Beijing showed that it arises mainly from secondary inorganic and organic aerosols, primary coal combustion and biomass burning emissions. The $PM_{2.5}$ source apportionment intercomparison shows that:

(1) For coal combustion, the time series of CMB and AMS/ACSM-PMF correlated well. Comparable concentration levels were only found for CMB and PMF in the winter.

(2) For biomass burning, the time series of CMB, PMF and AMS/ACSM-PMF correlated well, but the concentrations are only comparable at IAP during winter. The PMF results were problematic as biomass burning emissions are heavily overestimated.

(3) The average concentrations of traffic related particles were generally comparable for the different methods except at PG during winter.

(4) The cooking aerosol estimates by AMS/ACSM-PMF and CMB varied significantly. The secondary OM concentrations were comparable for CMB and

Open Access Article. Published on 23 2020. Downloaded on 09-10-2024 6:25:25.
This article is licensed under a Creative Commons Attribution 3.0 Unported Licence.

AMS/ACSM-PMF at IAP, but those at PG differed significantly. PMF did not resolve either cooking or secondary sources.

(5) The measured SNA concentration at IAP was higher than the SNA factor in PMF, but they were comparable at PG. The dust concentration in PMF was around 2–3 times that estimated in the CMB results, suggesting that at least one of the PMF dust factors is misassigned.

Our intercomparison exercise suggests that although there are some consistencies, the contributions of several sources modelled by CMB, PMF and AMS/ACSM-PMF differed significantly. The results from the CMB model appear to be both comprehensive and most consistent with those from other methods, whereas PMF did not work well with the APHH-Beijing dataset.

Author contributions

Z. S. and R. M. H. conceived the idea, J. X. conducted the method intercomparison and wrote the paper with the help of Z. S., R. M. H. and all co-authors. T. V. V. and D. L. conducted the aerosol sampling and laboratory-based chemical analyses. X. W. and J. X. conducted the CMB modelling at the PG and IAP sites, respectively. D. S. conducted the PMF modelling. A. V., V. M. and G. S. carried out the ^{14}C analysis. S. S. and A. S. H. P. supervised the ^{14}C analysis. S. H. conducted the analysis with the extended Gelencsér (EG) method incorporating ^{14}C data. Y. S. provided the AMS-PMF data. X. W. provided the ACSM-PMF data. All authors discussed the results and commented on this paper.

Conflicts of interest

The authors declare that they have no conflict of interest.

Acknowledgements

This research was funded by the Natural Environment Research Council (Grant No: NE/N007190/1, NE/R005281/1, NE/S006699/1). We thank Bill Bloss, Leigh Crilley, and Louisa Kramer from the University of Birmingham, Siyao Yue, Liangfang Wei, Hong Ren, Qiaorong Xie, Wanyu Zhao, Linjie Li, Ping Li, Shengjie Hou, and Qingqing Wang from the Institute of Atmospheric Physics, Rachel Dunmore, Ally Lewis, Jacqui Hamilton and James Lee from the University of York, Kebin He and Xiaoting Cheng from Tsinghua University, James Allan and Hugh Coe from the University of Manchester, Yiqun Han and Hanbing Zhang from King's College London, and Tong Zhu from Peking University for providing logistic and scientific support for the field campaigns. V. M. acknowledges the A. G. Leventis Foundation for a doctoral student Educational Grant.

References

1 B. Liu, N. Song, Q. Dai, R. Mei, B. Sui, X. Bi and Y. Feng, *Atmos. Res.*, 2016, **170**, 23–33.
2 R. Lyu, Z. Shi, M. S. Alam, X. Wu, D. Liu, T. V. Vu, C. Stark, R. Xu, P. Fu, Y. Feng and R. M. Harrison, *Atmos. Environ.*, 2019, **202**, 244–255.

Open Access Article. Published on 23 2020. Downloaded on 09-10-2024 6:25:25.
This article is licensed under a Creative Commons Attribution 3.0 Unported Licence.

3 Z. Shi, T. Vu, S. Kotthaus, R. M. Harrison, S. Grimmond, S. Yue, T. Zhu, J. Lee, Y. Han, M. Demuzere, R. E. Dunmore, L. Ren, D. Liu, Y. Wang, O. Wild, J. Allan, W. J. Acton, J. Barlow, B. Barratt, D. Beddows, W. J. Bloss, G. Calzolai, D. Carruthers, D. C. Carslaw, Q. Chan, L. Chatzidiakou, Y. Chen, L. Crilley, H. Coe, T. Dai, R. Doherty, F. Duan, P. Fu, B. Ge, M. Ge, D. Guan, J. F. Hamilton, K. He, M. Heal, D. Heard, C. N. Hewitt, M. Hollaway, M. Hu, D. Ji, X. Jiang, R. Jones, M. Kalberer, F. J. Kelly, L. Kramer, B. Langford, C. Lin, A. C. Lewis, J. Li, W. Li, H. Liu, J. Liu, M. Loh, K. Lu, F. Lucarelli, G. Mann, G. McFiggans, M. R. Miller, G. Mills, P. Monk, E. Nemitz, F. O'Connor, B. Ouyang, P. I. Palmer, C. Percival, O. Popoola, C. Reeves, A. R. Rickard, L. Shao, G. Shi, D. Spracklen, D. Stevenson, Y. Sun, Z. Sun, S. Tao, S. Tong, Q. Wang, W. Wang, X. Wang, X. Wang, Z. Wang, L. Wei, L. Whalley, X. Wu, Z. Wu, P. Xie, F. Yang, Q. Zhang, Y. Zhang, Y. Zhang and M. Zheng, *Atmos. Chem. Phys.*, 2019, **19**, 7519–7546.

4 J. Yin, S. A. Cumberland, R. M. Harrison, J. Allan, D. E. Young, P. I. Williams and H. Coe, *Atmos. Chem. Phys.*, 2015, **15**, 2139–2158.

5 J. G. Watson, J. C. Chow, D. H. Lowenthal, L. C. Pritchett, C. A. Frazier, G. R. Neuroth and R. Robbins, *Atmos. Environ.*, 1994, **28**, 2493–2505.

6 J. Yin, R. M. Harrison, Q. Chen, A. Rutter and J. J. Schauer, *Atmos. Environ.*, 2010, **44**, 841–851.

7 I. El Haddad, N. Marchand, H. Wortham, C. Piot, J. L. Besombes, J. Cozic, C. Chauvel, A. Armengaud, D. Robin and J. L. Jaffrezo, *Atmos. Chem. Phys.*, 2011, **11**, 2039–2058.

8 I. M. Ulbrich, M. R. Canagaratna, Q. Zhang, D. R. Worsnop and J. L. Jimenez, *Atmos. Chem. Phys.*, 2009, **9**, 2891–2918.

9 J. A. Engel-Cox and S. A. Weber, *J. Air Waste Manage. Assoc.*, 2007, **57**, 1307–1316.

10 A. Reff, S. I. Eberly and P. V. Bhave, *J. Air Waste Manage. Assoc.*, 2007, **57**, 146–154.

11 S. G. Brown, S. Eberly, P. Paatero and G. A. Norris, *Sci. Total Environ.*, 2015, **518–519**, 626–635.

12 M. R. Canagaratna, J. T. Jayne, J. L. Jimenez, J. D. Allan, M. R. Alfarra, Q. Zhang, T. B. Onasch, F. Drewnick, H. Coe, A. Middlebrook, A. Delia, L. R. Williams, A. M. Trimborn, M. J. Northway, P. F. DeCarlo, C. E. Kolb, P. Davidovits and D. R. Worsnop, *Mass Spectrom. Rev.*, 2007, **26**, 185–222.

13 S. H. Budisulistiorini, M. R. Canagaratna, P. L. Croteau, W. J. Marth, K. Baumann, E. S. Edgerton, S. L. Shaw, E. M. Knipping, D. R. Worsnop, J. T. Jayne, A. Gold and J. D. Surratt, *Environ. Sci. Technol.*, 2013, **47**, 5686–5694.

14 W. Xu, Y. Sun, Q. Wang, J. Zhao, J. Wang, X. Ge, C. Xie, W. Zhou, W. Du, J. Li, P. Fu, Z. Wang, D. R. Worsnop and H. Coe, *J. Geophys. Res.: Atmos.*, 2019, **124**, 1132–1147.

15 N. Takegawa, Y. Miyazaki, Y. Kondo, Y. Komazaki, T. Miyakawa, J. L. Jimenez, J. T. Jayne, D. R. Worsnop, J. D. Allan and R. J. Weber, *Aerosol Sci. Technol.*, 2005, **39**, 760–770.

16 D. A. Day, S. Liu, L. M. Russell and P. J. Ziemann, *Atmos. Environ.*, 2010, **44**, 1970–1979.

17 M. Crippa, F. Canonaco, V. A. Lanz, M. Äijälä, J. D. Allan, S. Carbone, G. Capes, D. Ceburnis, M. Dall'Osto, D. A. Day, P. F. DeCarlo, M. Ehn, A. Eriksson, E. Freney, L. Hildebrandt Ruiz, R. Hillamo, J. L. Jimenez, H. Junninen,

Open Access Article. Published on 23 2020. Downloaded on 09-10-2024 6:25:25.
This article is licensed under a Creative Commons Attribution 3.0 Unported Licence.

A. Kiendler-Scharr, A. M. Kortelainen, M. Kulmala, A. Laaksonen, A. A. Mensah, C. Mohr, E. Nemitz, C. O'Dowd, J. Ovadnevaite, S. N. Pandis, T. Petäjä, L. Poulain, S. Saarikoski, K. Sellegri, E. Swietlicki, P. Tiitta, D. R. Worsnop, U. Baltensperger and A. S. H. Prévôt, *Atmos. Chem. Phys.*, 2014, **14**, 6159–6176.

18 C. Mohr, J. A. Huffman, M. J. Cubison, A. C. Aiken, K. S. Docherty, J. R. Kimmel, I. M. Ulbrich, M. Hannigan and J. L. Jimenez, *Environ. Sci. Technol.*, 2009, **43**, 2443–2449.

19 L. Xu, S. Suresh, H. Guo, R. J. Weber and N. L. Ng, *Atmos. Chem. Phys.*, 2015, **15**, 7307–7336.

20 Y. L. Zhang, R. J. Huang, I. El Haddad, K. F. Ho, J. J. Cao, Y. Han, P. Zotter, C. Bozzetti, K. R. Daellenbach, F. Canonaco, J. G. Slowik, G. Salazar, M. Schwikowski, J. Schnelle-Kreis, G. Abbaszade, R. Zimmermann, U. Baltensperger, A. S. H. Prévôt and S. Szidat, *Atmos. Chem. Phys.*, 2015, **15**, 1299–1312.

21 P. Zotter, V. G. Ciobanu, Y. L. Zhang, I. El-Haddad, M. Macchia, K. R. Daellenbach, G. A. Salazar, R. J. Huang, L. Wacker, C. Hueglin, A. Piazzalunga, P. Fermo, M. Schwikowski, U. Baltensperger, S. Szidat and A. S. H. Prévôt, *Atmos. Chem. Phys.*, 2014, **14**, 13551–13570.

22 Y.-L. Zhang, J. Li, G. Zhang, P. Zotter, R.-J. Huang, J.-H. Tang, L. Wacker, A. S. H. Prévôt and S. Szidat, *Environ. Sci. Technol.*, 2014, **48**, 2651–2659.

23 R. J. Sheesley, E. Kirillova, A. Andersson, M. Kruså, P. S. Praveen, K. Budhavant, P. D. Safai, P. S. P. Rao and Ö. Gustafsson, *J. Geophys. Res.: Atmos.*, 2012, **117**, D10202.

24 L. A. Currie, *Radiocarbon*, 2000, **42**, 115–126.

25 S. Szidat, T. M. Jenk, H. W. Gäggeler, H. A. Synal, R. Fisseha, U. Baltensperger, M. Kalberer, V. Samburova, S. Reimann, A. Kasper-Giebl and I. Hajdas, *Atmos. Environ.*, 2004, **38**, 4035–4044.

26 C. M. Reddy, A. Pearson, L. Xu, A. P. McNichol, B. A. Benner, S. A. Wise, G. A. Klouda, L. A. Currie and T. I. Eglinton, *Environ. Sci. Technol.*, 2002, **36**, 1774–1782.

27 A. S. Holden, A. P. Sullivan, L. A. Munchak, S. M. Kreidenweis, B. A. Schichtel, W. C. Malm and J. L. Collett, *Atmos. Environ.*, 2011, **45**, 1986–1993.

28 J. Liu, J. Li, Y. Zhang, D. Liu, P. Ding, C. Shen, K. Shen, Q. He, X. Ding, X. Wang, D. Chen, S. Szidat and G. Zhang, *Environ. Sci. Technol.*, 2014, **48**, 12002–12011.

29 S. Szidat, M. Vonwiller, G. A. Salazar Quintero, W. W. Hu, J. L. Jimenez, E. Edgerton, S. Shaw and A. S. H. Prevot, *Presented in part at the 10th International Aerosol Conference (IAC 2018)*, St. Louis, Missouri, USA, 2018.

30 L. Ke, X. Ding, R. L. Tanner, J. J. Schauer and M. Zheng, *Atmos. Environ.*, 2007, **41**, 8898–8923.

31 X.-F. Huang, L. Xue, X.-D. Tian, W.-W. Shao, T.-L. Sun, Z.-H. Gong, W.-W. Ju, B. Jiang, M. Hu and L.-Y. He, *Atmos. Environ.*, 2013, **64**, 200–207.

32 K. R. Bullock, R. M. Duvall, G. A. Norris, S. R. McDow and M. D. Hays, *Atmos. Environ.*, 2008, **42**, 6897–6904.

33 S. S. Steimer, D. J. Patton, T. V. Vu, M. Panagi, P. S. Monks, R. M. Harrison, Z. L. Fleming, Z. Shi and M. Kalberer, *Atmos. Chem. Phys. Discuss.*, 2020, **2020**, 1–26.

Open Access Article. Published on 23 2020. Downloaded on 09-10-2024 6:25:25.
This article is licensed under a Creative Commons Attribution 3.0 Unported Licence.

34 Y. L. Zhang, N. Perron, V. G. Ciobanu, P. Zotter, M. C. Minguillón, L. Wacker, A. S. H. Prévôt, U. Baltensperger and S. Szidat, *Atmos. Chem. Phys.*, 2012, **12**, 10841–10856.
35 S. Szidat, G. A. Salazar, E. Vogel, M. Battaglia, L. Wacker, H.-A. Synal and A. Türler, *Radiocarbon*, 2014, **56**, 561–566.
36 J. Xu, D. Liu, X. Wu, T. V. Vu, Y. Zhang, P. Fu, Y. Sun, W. Xu, D. Ji, R. M. Harrison and Z. Shi, *Atmos. Chem. Phys.*, 2020, under review.
37 X. Wu, C. Chen, T. V. Vu, D. Liu, C. Baldo, X. Shen, Q. Zhang, K. Cen, M. Zheng, K. He, Z. Shi and R. M. Harrison, *Environ. Pollut.*, 2020, **266**(1), 115078.
38 A. Gelencsér, B. May, D. Simpson, A. Sánchez-Ochoa, A. Kasper-Giebl, H. Puxbaum, A. Caseiro, C. Pio and M. Legrand, *J. Geophys. Res.: Atmos.*, 2007, **112**, D23S04.
39 S. Hou, D. Liu, J. Xu, T. V. Vu, X. Wu, D. Srivastava, P. Fu, Y. Sun, A. Vlachou, V. Moschos, G. Salazar, S. Szidat, A. S. H. Prévôt, Z. Shi and R. M. Harrison, *Atmos. Chem. Phys.*, 2020, under review.
40 P. Paatero and U. Tapper, *Environmetrics*, 1994, **5**, 111–126.
41 D. Srivastava, J. Xu, D. Liu, T. V. Vu, Z. Shi and R. M. Harrison, *Atmos. Chem. Phys.*, 2020.
42 D. Liu, M. Vonwiller, J. Li, J. Liu, S. Szidat, Y. Zhang, C. Tian, Y. Chen, Z. Cheng, G. Zhong, P. Fu and G. Zhang, *Aerosol Air Qual. Res.*, 2020, **20**, 2495–2506.
43 Y. Guo, *Environ. Sci. Pollut. Res.*, 2016, 13918–13930.
44 H. Ni, R. J. Huang, J. Cao, W. Liu, T. Zhang, M. Wang, H. A. J. Meijer and U. Dusek, *Atmos. Chem. Phys.*, 2018, **18**, 16363–16383.
45 M. Xie, M. D. Hays and A. L. Holder, *Sci. Rep.*, 2017, **7**, 7318.
46 E. Reyes-Villegas, T. Bannan, M. Le Breton, A. Mehra, M. Priestley, C. Percival, H. Coe and J. D. Allan, *Environ. Sci. Technol.*, 2018, **52**, 5308–5318.
47 D. Srivastava, O. Favez, J. E. Petit, Y. Zhang, U. M. Sofowote, P. K. Hopke, N. Bonnaire, E. Perraudin, V. Gros, E. Villenave and A. Albinet, *Sci. Total Environ.*, 2019, **690**, 944–955.
48 D. Hoffmann, A. Tilgner, Y. Iinuma and H. Herrmann, *Environ. Sci. Technol.*, 2010, **44**, 694–699.
49 X. Zhao, Q. Hu, X. Wang, X. Ding, Q. He, Z. Zhang, R. Shen, S. Lü, T. Liu, X. Fu and L. Chen, *J. Atmos. Chem.*, 2015, **72**, 1–18.
50 Y. Sun, W. Du, P. Fu, Q. Wang, J. Li, X. Ge, Q. Zhang, C. Zhu, L. Ren, W. Xu, J. Zhao, T. Han, D. R. Worsnop and Z. Wang, *Atmos. Chem. Phys.*, 2016, **16**, 8309–8329.
51 M. Elser, R. J. Huang, R. Wolf, J. G. Slowik, Q. Wang, F. Canonaco, G. Li, C. Bozzetti, K. R. Daellenbach, Y. Huang, R. Zhang, Z. Li, J. Cao, U. Baltensperger, I. El-Haddad and A. S. H. Prévôt, *Atmos. Chem. Phys.*, 2016, **16**, 3207–3225.
52 K. L. Abdullahi, J. M. Delgado-Saborit and R. M. Harrison, *Atmos. Environ.*, 2018, **178**, 282–285.
53 J. C. Chow, D. H. Lowenthal, L. W. A. Chen, X. L. Wang and J. G. Watson, *Air Qual., Atmos. Health*, 2015, **8**, 243–263.
54 Y. Sun, Y. He, Y. Kuang, W. Xu, S. Song, N. Ma, J. Tao, P. Cheng, C. Wu, H. Su, Y. Cheng, C. Xie, C. Chen, L. Lei, Y. Qiu, P. Fu, P. Croteau and D. R. Worsnop, *Geophys. Res. Lett.*, 2020, **47**, e2019GL086288.
55 J. Xu, S. Song, R. M. Harrison, C. Song, L. Wei, Q. Zhang, Y. Sun, L. Lei, C. Zhang, X. Yao, D. Chen, W. Li, M. Wu, H. Tian, L. Luo, S. Tong, W. Li,

J. Wang, G. Shi, Y. Huangfu, Y. Tian, B. Ge, S. Su, C. Peng, Y. Chen, F. Yang, A. Mihajlidi-Zelić, D. Đorđević, S. J. Swift, I. Andrews, J. F. Hamilton, Y. Sun, A. Kramawijaya, J. Han, S. Saksakulkrai, C. Baldo, S. Hou, F. Zheng, K. R. Daellenbach, C. Yan, Y. Liu, M. Kulmala, P. Fu and Z. Shi, *Atmos. Meas. Tech. Discuss.*, 2020, **2020**, 1–36.

56 D. K. Farmer, A. Matsunaga, K. S. Docherty, J. D. Surratt, J. H. Seinfeld, P. J. Ziemann and J. L. Jimenez, *Proc. Natl. Acad. Sci. U. S. A.*, 2010, **107**, 6670–6675.

57 Y. Liu, M. Zheng, M. Yu, X. Cai, H. Du, J. Li, T. Zhou, C. Yan, X. Wang, Z. Shi, R. M. Harrison, Q. Zhang and K. He, *Atmos. Chem. Phys.*, 2019, **19**, 6595–6609.

Open Access Article. Published on 23 2020. Downloaded on 09-10-2024 6:25:25.
This article is licensed under a Creative Commons Attribution 3.0 Unported Licence.